Conditional toxicity and synergy drive diversity among antibacterial effectors

Kaitlyn D. LaCourse[1], **S. Brook Peterson**[1], **Hemantha D. Kulasekara**[1], **Matthew C. Radey**[1], **Jungyun Kim**[1], and **Joseph D. Mougous**[1,2,*]

[1]Department of Microbiology, University of Washington, Seattle, WA 98195, USA

[2]Howard Hughes Medical Institute, University of Washington, Seattle, WA 98195, USA

Abstract

Bacteria in polymicrobial habitats contend with a persistent barrage of competitors, often under rapidly changing environmental conditions[1]. The direct antagonism of competitor cells is thus an important bacterial survival strategy[2]. Towards this end, many bacterial species employ an arsenal of antimicrobial effectors with multiple activities; however, the benefits conferred by the simultaneous deployment of diverse toxins are unknown. Here we show that the multiple effectors delivered to competitor bacteria by the type VI secretion system (T6SS) of *Pseudomonas aeruginosa* display conditional efficacy and act synergistically. One of these effectors, Tse4, is most active in high salinity environments and synergizes with effectors that degrade the cell wall or inactivate intracellular electron carriers. We find Tse4 synergizes with these disparate mechanisms by forming pores that disrupt the Ψ component of the proton motive force. Our results provide evidence that the concomitant delivery of a cocktail of effectors serves as a bet-hedging strategy to promote bacterial competitiveness in the face of unpredictable and variable environmental conditions.

The T6SS is a functionally plastic pathway that is used by many bacteria to translocate toxic effector proteins into adjacent cells[3–6]. Effectors that target bacteria generally degrade conserved, essential cellular structures, and as such, single effectors are sufficient to kill or terminate growth[7,8]. Despite the capacity of single effectors to kill target cells, the γ-proteobacterium *P. aeruginosa* delivers a diverse cocktail of effectors that degrade, among other structures, phospholipids, peptidoglycan, and nicotinamide adenine dinucleotides[9–11]. The T6SSs of other experimentally characterized bacteria also deliver effectors that target multiple essential molecules[7,12]. To estimate the generality of this phenomenon, we searched the genomes of 2566 sequenced Proteobacterial species for T6SS effectors with known activities. Only 42% (n=474) of the species within this group that contain the T6SS also

*To whom correspondence should be addressed: J.D.M. mougous@u.washington.edu, Telephone – (+1) 206-685-7742.

contain an effector of known activity, suggesting that many as yet undescribed effectors exist. Nevertheless, we found that 40% (n=196) of these species possess a second effector with unique biochemical activity, and 25% (n=52) possess three or more (Supplementary Table 1). Such bacteria were identified in four of the five major classes of Proteobacteria (Fig. 1). These data suggest that bacteria benefit from the coordinated delivery of effectors with diverse biochemical activities.

We considered the potential benefits that could select for and maintain a diversity of T6SS effectors. Utilizing multiple antibiotic mechanisms simultaneously is a well-documented strategy for minimizing the evolution of resistance[13]. This strategy might also overcome potential intrinsic resistance mechanisms present in the wide phylogenetic range of bacteria targeted by the T6SS. While preventing resistance may contribute to effector expansion, due to the essentiality and structural conservation of T6SS effector targets, we reasoned it is unlikely to be the major selective pressure driving the extent of effector diversity observed.

Two additional benefits conferred by a diverse effector arsenal could be that the toxins act with synergy on recipient cells or that they display conditional efficacy. The former is defined by instances in which the activity of two or more effectors on recipient cells is greater than the sum of their individual activities, whereas the latter is defined by effectors that contribute to recipient cell intoxication in a manner dependent on the environmental conditions. Synergy and conditional efficacy among T6 effectors have not been explored, and we reasoned that both offered a potential explanation for the effector diversity observed. It is worth noting that these scenarios are not mutually exclusive.

To interrogate T6 effectors in a high-throughput fashion, we developed a sequencing-based, pooled strategy for measuring their activity during interbacterial competition (Fig. 2a-c). Henceforth, we refer to this method as PAEE (Parallel Analysis of Effector Efficacy). Briefly, we introduced unique barcode sequences to a library of *P. aeruginosa* strains rendered susceptible to intoxication by one or two effectors of the Hcp Secretion Island I-encoded T6SS (H1-T6SS) through the deletion of effector–immunity gene pairs. Thus, only effectors with an experimentally defined cognate immunity determinant were included (Tse1-6). Prior studies established the antibacterial activity of these effectors, though the precise biochemical mechanisms of Tse2, Tse4 and Tse5 remain unknown (Fig. 2a). A pool containing the barcoded mutants and a barcoded toxin-resistant reference strain was then cultivated under a variety of conditions with an excess of the unmarked parental strain acting as a toxin donor. Susceptibility to intoxication was assessed by comparing the frequency of the barcode associated with a given mutant to the reference strain at the beginning and end of the experiment (Fig. 2b,c). To uncouple the potential contribution of regulation from the inherent biochemical capacity of effectors to act synergistically or conditionally, we utilized a background of *P. aeruginosa* (retS) in which Tse1-6 are produced constitutively[14]. Data presented herein derive from four independent repetitions of PAEE.

Prolonged cell–cell contact is critical for T6SS-mediated effector translocation[15]. Conditions that do not permit extended contact, such as cultivation on semi-solid surfaces or in liquid, thus provide a convenient means of specifically evaluating the contribution of the T6SS to fitness[4]. Consistent with this, we found that our barcoded effector-susceptible strains

displayed fitness defects only when cultivated under T6S-conducive conditions (Supplementary Fig. 1). Moreover, we noted that the relative magnitude of individual effector activities under T6S-conductive conditions approximated those observed in earlier studies. With this validation of our method, we sought to examine whether T6SS effectors display conditional efficacy. We measured effector activity under growth conditions varying in parameters that are likely in flux across the environmental habitats where *P. aeruginosa* resides, including salinity, temperature, oxygen availability and pH. PAEE identified several conditions in which the relative efficacy of effectors varied compared to a reference condition, including high salinity, anaerobiosis, high temperature, and alkalinity (Fig. 2d-g). For instance, between pH 6 and pH 8, the relative activity of Tse5 increases seven-fold, whereas that of Tse3 decreases by 50%. Importantly, these results reproduced in pairwise interbacterial competition assays (Supplementary Fig. 2). In total, we observed that the efficacy of each of the six effectors examined can be significantly altered between one or more of the conditions examined.

Next we used PAEE to ask whether effectors can act synergistically. We found striking differences in the capacity of, and frequency by which effector pairs exhibit this behavior (Fig. 3a-d, and Supplementary Fig. 3a-k). For example, the cumulative activity of Tse3 and Tse4 exceeds the sum of the two individual effectors in all conditions tested (Fig. 3a). On the contrary, we did not observe an instance of synergy between Tse2 and Tse4 (Fig. 3b). We found that effector pair synergy can also be conditional. For example, synergy between Tse1 and Tse4 was most pronounced in high salinity and synergy between Tse2 and Tse6 was detected only in anaerobiosis (Fig. 3c and Supplementary Fig. 3g). Though infrequent, we found that the cumulative activity of two effectors can be less than that of the most active of the two effectors alone. In these instances, intoxication by one effector apparently diminishes the potency of the other. The majority of effector pairs did not exhibit this inhibition; however, the cumulative activity of Tse4 and Tse5 was at or below that of the more active single effector under most conditions analyzed (Fig. 3d). Pairwise co-cultivation experiments validated instances of each category of behavior observed by an effector–immunity pair in our PAEE screen (Supplementary Fig. 3l). Finally, we noted that effectors of *P. aeruginosa* do not equally participate in synergistic interactions; only Tse1, Tse4 and Tse6 were members of multiple strongly synergistic pairs (Fig. 3e). Together, these data indicate the capacity for T6SS effectors to act both conditionally and synergistically.

The genetic background employed in PAEE enforces constitutive effector production, which minimizes the potential impact of regulatory inputs. To understand the potential for effector expression to affect conditional toxicity and synergy, we measured the expression of *tse*1-6 in wild-type *P. aeruginosa* under conditions matching those used above. Consistent with previous data, we found that effector expression levels are positively correlated with genes encoding the T6S apparatus (p=0.03). Interestingly, we did not find that the expression of effectors is generally elevated under conditions optimal for their intrinsic activity (Fig. 3f). These data suggest that conditional effector efficacy in *P. aeruginosa* is achieved primarily by the conditional nature of intrinsic effector mechanisms rather than by differential regulation.

One of the findings to emerge from our PAEE screening is that an effector of unknown function, Tse4, acts in a synergistic fashion with peptidoglycan-targeting effectors Tse1 and Tse3, and the NAD$^+$ glycohydrolase Tse6 (Fig. 2a, Fig. 3a,c and Supplementary Fig. 3j). To understand how the activity of a single effector synergizes with the disruption of such disparate cellular processes, we investigated the mechanism of action of Tse4. Previous studies established that Tse4 must localize to the periplasm in order to exert toxicity[16]; however, the toxin bears no homology to characterized proteins that act in this compartment.

As a first step toward characterizing Tse4, we examined the phenotypic consequences of Tse4 delivery to a sensitive strain during interbacterial growth competition. Intoxication by Tse4 promoted growth inhibition without an apparent diminishment of viability, indicative of a bacteriostatic mechanism (Fig. 4a). Our PAEE screens revealed that high salinity enhances Tse4-based toxicity (Fig. 2e). To gain further insights into the mechanism of Tse4, we tested whether the conditional efficacy of the toxin derives from its induction of specific ion sensitivity or from a more general inability of intoxicated cells to withstand high osmolarity. For these studies, we generated a strain of *P. aeruginosa* (*tsi4*) capable of self-intoxication via Tse4. When grown under contact-promoting conditions, this strain displayed a profound, T6S-dependent growth defect on media containing sodium chloride (150 mM) or lithium chloride (20 mM) at concentrations sub-inhibitory to the wild-type (Fig. 4b). In contrast, significant growth inhibition was not observed on media containing potassium chloride or sucrose at levels equiosmolar to that of sodium chloride. These data suggest that Tse4 activity promotes sensitivity to monovalent cations and they explain the enhanced efficacy of Tse4 under conditions of high salinity observed by PAEE.

As observed for all T6SS effector–immunity pairs characterized to-date, we found that Tse4 and its cognate immunity determinant, Tsi4, interact directly (Supplementary Fig. 4a). Both possess predicted transmembrane domains and a prior study demonstrated that the proteins localize to the inner membrane of *P. aeruginosa* (Supplementary Fig. 4b)[17]. Tse4 is also characterized by a high content of glycine residues, many of which are in configurations reminiscent of glycine zipper motifs (Supplementary Fig. 4c). These sequences can promote multimerization of transmembrane segments and frequently occur in proteins that induce pores, including bacterial toxins[18]. To test the importance of these residues for Tse4 function, we generated a panel of mutants in which glycine residues predicted to form a transmembrane glycine zipper were substituted for valine. All of these mutants exhibited decreased Tse4-mediated intercellular intoxication (Supplementary Fig. 4d). Substitutions at G176 and G184 also impacted Tse4 secretion and stability, thereby complicating interpretation of the intoxication defects of these alleles (Supplementary Fig. 4e). However, proteins containing G180V or G186V substitutions were produced and secreted at wild-type levels, indicating specific disruption of toxin activity. Alleles encoding substitutions in adjacent non-glycine residues (A187V and A188V) had no impact on Tse4 function despite diminished secretion. These observations, taken together with the ion sensitivity we found is induced by Tse4, led us to hypothesize that the effector forms pores in the inner membrane of intoxicated cells.

Bacteria concentrate potassium ions in their cytoplasm and thus its release to the milieu is a convenient measure of membrane pore formation. Therefore, we monitored potassium

release from Tse4-intoxicated cells using inductively-coupled plasma optical emission spectroscopy. One hour after Tse4 induction, the level of extracellular potassium detected from a strain lacking Tsi4 approached that of mechanically lysed cells (Fig. 4c). Immunity to Tse4 inhibited the accumulation of extracellular potassium and allowed cells to concentrate potassium intracellularly during this period. We next asked whether the action of Tse4 allows the translocation of larger, organic molecules. Neither propidium iodide (668 Da) nor *o*-nitrophenyl-β-galactopyranoside (301 Da) accessed the cytoplasm of Tse4-intoxicated cells (Fig. 4d). However, control cells treated with pyocin S5, a bacterial toxin previously shown to form large, non-selective pores, were permeable to both molecules. In summary, these findings suggest that Tse4 induces membrane pores that accommodate ions, but exclude larger organic molecules.

Tse4 induction leads to bacteriostasis and the permeability of the inner membrane to ions, suggesting that the toxin disrupts the proton motive force (PMF). To measure the Ψ component of the PMF, we used the membrane potential-sensitive fluorescent dye $DiOC_2(3)$[19]. Tse4 intoxication resulted in a dramatic decrease in Ψ, nearly to the level of the ionophore-treated control (Fig. 4e). In contrast, by employing the pH-sensitive green fluorescent protein pHluorin2[20], we found that Tse4-intoxicated cells have no defect in the maintenance of the pH component of the PMF (Fig. 4f). It is noteworthy that this result is consistent with our PAEE findings, which indicated that the efficacy of Tse4 is enhanced by sodium ions, but unaffected by changes in pH. In total, our data indicate that Tse4 promotes highly selective membrane permeability. Although we cannot definitively rule-out alternate mechanisms by which Tse4 may act, the most parsimonious explanation for our findings is that Tse4 acts by facilitating the formation of ion selective membrane pores. Synergy between Tse4 and cell wall-degrading effectors (Tse1, Tse3) may be achieved by activation of PMF-sensitive autolysins[21]. Likewise, Tse4 could exacerbate the consequences of NAD^+ depletion (Tse6) by inhibiting transporters that rely on Ψ to maintain cellular homeostasis.

Our analyses reveal the benefits to bacteria of maintaining a biochemically diverse effector repertoire. In the rapidly changing and unpredictable surroundings characteristic of life at the micron scale, the concomitant delivery of multiple effectors with a range of conditional optima may act as a bet hedging strategy. As a corollary, the set of effectors a bacterium possesses should provide a window into the environmental conditions in which it encounters competitors. The benefits conferred by the delivery of toxins with conditional and synergistic activities underscores the utility of combination antibiotic therapy beyond the subversion of resistance[22].

Methods

Bacterial strains, plasmids, and growth conditions

A detailed list of all strains and plasmids created in this study can be found in Supplementary Tables 2 and 3. All *P. aeruginosa* strains were derived from the sequenced strain PAO1[23] and were grown on Luria-Bertaini (LB) medium at 37°C supplemented as appropriate with 30 μg ml^{-1} gentamicin, 25 μg ml^{-1} irgasan, 75 μg ml^{-1} tetracycline, 5% (*w/v*) sucrose, 0.2 mM IPTG (isopropyl β-D-1-thiogalactopyranoside), 0.02% (*w/v*) arabinose, and 40 μg ml^{-1} X-gal (5-bromo-4-chloro-3-indolyl β-D-galactopyranoside).

Escherichia coli was grown in LB medium supplemented as appropriate with 15 μg ml^{-1} gentamicin, and 0.2 mM IPTG. *E. coli* strains DH5α, BL21(DE3), and SM10 (Novagen, Hornsby Westfield, Australia) were used for plasmid maintenance, gene expression, and conjugative transfer, respectively. Plasmids pPSV39-CV and pETDuet-1 were used for inducible expression in *P. aeruginosa* and *E. coli* respectively. Site-specific chromosomal insertions in *P. aeruginosa* were generated using pUC18-Tn7t-pBAD-*araE* (*glmS*) or pMiniCtx-1 (*attB*) as previously described[24,25].

Bioinformatic search for type VI effectors encoded by Proteobacteria

We generated custom Hidden Markov Model (HMM) profiles for experimentally validated effectors and a T6S structural gene (*tssC*) from homolog alignments using hmmscan from the HMMER 3.1b2 tool set. The effectors groups chosen for this search were: Tae1, Tae2, Tae3, Tae4, Tge1, Tge2, Tge3, Tle1, Tle2, Tle3, Tle4, Tle5, VasX and Tse4, as well as proteins containing Tox46 (NAD(P)$^+$ glycohydrolase) and Tox34 (HNH DNase) motifs[10,11,26–29]. For all Proteobacterial species on the List of Prokaryotic names with Standing in Nomenclature (LPSN, http://www.bacterio.net/), a strain was selected at random and the corresponding genome downloaded from the NCBI complete genome database. Draft genomes were selected and translated if no complete genomes were available. These genomes were searched for proteins matching our custom HMM profiles. Results were binned by profile hits and filtered using E-value cut-offs. Appropriate cut-off values were selected by manually identifying the highest value for a given sequence that was found in the appropriate genomic context. For effectors, this included proximity of immunity gene candidates, *vgrG* homologs, and genes encoding accessory proteins with T6S-related domains of unknown function. Hits for *tssC* were validated by identifying adjacent genes encoding other T6S structural components.

Parallel analysis of effector efficacy screen (PAEE)

Generation of barcoded mutant strains—The pEXG2 suicide vector was used for creating in-frame chromosomal deletions in *P. aeruginosa* as previously described[30]. Single and pairwise deletions of the six H1-T6SS effector–immunity gene pairs in *P. aeruginosa* was used to generate 21 different strains (see Fig. 1 and Supplementary Table 2). The integration vector mini-CTX1 was then used to insert a unique 18 base pair barcode at the neutral phage attachment site B (*attB*) in each mutant as well as the wild-type parent strain[24]. Finally, allelic exchange employing pEXG2 was used to introduce an in-frame deletion of *retS* in each barcoded strain.

Bacterial growth competitions—The 22 barcoded strains were grown for 16 hours on LB no salt (LBNS) medium agar plates, then resuspended in LBNS broth before pooling together at equal concentrations (normalized to OD$_{600}$ 0.2) and mixed with an excess of a donor (*P. aeruginosa* PAO1 *retS*, donor to recipient= 10:1). This mixture (5 μl) was spotted on a 0.2 μm nitrocellulose membrane placed on 3% (*w/v*) agar plates, except as noted in Supplementary Table 4. Plate composition, incubation times and other varied growth conditions are described in Supplementary Table 4. After the incubation period noted in Supplementary Table 4, competitions were harvested into LBNS broth and washed twice with the same medium. Cells were then incubated with 10 mg/mL benzonase (Sigma-

Aldrich, St. Louis, MO) for 30 min at 37°C to remove extracellular DNA, and washed a final time with LBNS medium containing 5 mM EDTA to inactivate the benzonase.

Sequencing—Total DNA was extracted from washed, benzonase treated cells using the DNeasy kit (Qiagen, Hilden, Germany). The barcode region was amplified using primers containing an adaptor sequence and targeting conserved regions flanking the integrated barcodes. Amplification was monitored via SYBR Green incorporation and terminated prior to saturation. A second round of amplification was used to introduce Nexterra sequencing adapters (Illumina, San Deigo, CA) and unique indices for each library, and sequencing was performed using an Illumina MiSeq instrument (50 cycles program).

Analysis—Each read was assessed for an exact match at the barcode position using string matching, with no mismatches for any base allowed and excluding reverse complemented matches (reads that did not meet these criteria were filtered). To normalize values between different conditions, we converted the reads for each barcoded strain into a fraction of the total reads for each individual condition. Effector activity (E_a) was calculated by a metric analogous to a competitive index using the following equation:

$$E_a = \log\left(\frac{Final\left(\frac{parent}{mutant}\right)}{Initial\left(\frac{parent}{mutant}\right)}\right)$$

Synergy was calculated as the observed activity of an effector pair compared to the expected additive value (observed/expected, o/e). The expected additive value is the sum of the individual effector activities from single effector susceptible barcoded strains minus 1. Synergy was defined as any o/e value>1, meaning the activity of the effector pair was greater than the sum of its individual effector activities. The bar for inhibition was calculated as the percent contribution of the most active effector within the pair to the expected additive value. Partially additive activity was defined by o/e values greater than the inhibitory cutoff and <1.

Effector expression analysis

Expression of T6SS effector and structural genes was measured in wild-type *P. aeruginosa* PAO1. Cultures were grown for 16 hrs in LB broth, then cells (5 μL) were spotted on 0.2 μm nitrocellulose filters placed upon agar plates. Agar plate composition and incubation conditions are the same as employed in PAEE (Supplementary Table 4). Spots were harvested from nitrocellulose and resuspended into Bacterial RNA Protect buffer (Qiagen). Cells were lysed by lysozyme treatment (1 mg/ml for 10 min) followed by sonication. RNA was purified using the RNeasy kit (Qiagen), residual DNA removed by Turbo DNAse (Invitrogen), and remaining RNA purified and concentrated using the RNA Minelute kit (Qiagen). cDNA was synthesized using the High Capacity cDNA Reverse Transcription Kit (Thermo Fisher, Watham, MA). Gene expression was measured using SYBR Green-based quantitative PCR with primers targeting each gene of interest, and normalized to the housekeeping gene *rpoD*. Primer sequences are available upon request. Two independent experiments with three technical replicates included were performed for each measurement.

Growth competition assays

For *P. aeruginosa* competitions, the recipient strain contained *lacZ* (tetracycline-resistant) inserted at the neutral phage attachment site (*attB*) to enable its differentiation or selection from the unlabeled donor strain when plated on LB containing X-gal (40 μg ml^{-1}) or tetracycline (75 μg ml^{-1}). Overnight cultures of donor and recipient strains were washed, OD$_{600}$ standardized, and mixed at the ratios indicated. Competition mixtures (5 μl) were then spotted in triplicate on a 0.2 μm nitrocellulose membrane overlaid on a 3% (*w/v*) agar plate of the indicated media and incubated face up at 37°C for 8 hrs unless denoted otherwise. Competitions were harvested from the nitrocellulose membrane and resuspended into LB medium. Initial and final populations of donor and recipient cells were enumerated following serial dilution on appropriate selective or differentiation media. The competitive index (CI) is defined as:

$$CI = \frac{Final\left(\frac{donor\ c.f.u.}{recipient\ c.f.u.}\right)}{Initial\left(\frac{donor\ c.f.u.}{recipient\ c.f.u.}\right)}$$

P. aeruginosa toxicity assays

For toxicity assays, overnight cultures of *P. aeruginosa* expressing mCherry from a neutral site chromosomal gene insertion (attTn7::*mCherry*) were normalized to an OD$_{600}$ of 1, diluted in 10-fold increments, and each dilution was spotted onto LBNS 3% (*w/v*) agar plates supplemented with the indicated solutes. Plates were incubated 16 hours at 37°, then fluorescence was imaged using a FluorChem Q imaging system (Protein Simple).

Potassium release assays

P. aeruginosa strains were grown overnight in a low K$^+$ media (10 mM bis-tris propane pH 7.0, 5 mM succinate, 2 mM MgCl$_2$, 5 mM (NH$_4$)$_2$SO$_4$, 1 mM Na$_2$HPO$_4$, 10 μM Fe(NH$_4$)SO$_4$, 0.1% (*w/v*) tryptone, 0.005% (*w/v*) yeast extract). Overnight cultures were back diluted 1:100 in low K$^+$ media, grown to mid-log phase, pelleted by centrifugation at room temperature, and the OD$_{600}$ set to 2 in a 5 mL volume of low K$^+$ medium. Cultures were then induced with 0.02% (*w/v*) arabinose for the indicated times, cells were pelleted by centrifugation, and the supernatant collected and sterilized through a 0.2 μm cellulose acetate membrane filter (VWR, Radnor, PA). As a positive control for maximal potassium release, cells were lysed by sonication and subsequent boiling. Potassium measurements were performed by inductively coupled plasma-optical emission spectrometry (ICP-OES Optima 8300, Perkin Elmer, Waltham, MA) operating both 766.4 and 404.7 nm emission lines. Data were calibrated with a potassium standard (Sigma-Aldrich).

Cytoplasmic membrane permeability assays

Propidium iodide (668.4 Daltons)—Overnight cultures of *P. aeruginosa* strains were diluted 1:100 in LB medium, grown to mid-log phase, and induced for one hour with 0.02% (*w/v*) arabinose or incubated with the pore-forming protein control (5 μg/mL pyocin S5). Cells were collected by centrifugation and washed twice with 1 mL phosphate buffer saline (PBS, pH 7.1). Bacterial cells equivalent to 1 mL at OD$_{600}$=1 were incubated with 5 μg/mL

propidium iodide in the dark for 10 min, then fluorescence was measured at (ex. 353 nm/em. 353 nm).

ONPG (301.3 Daltons)—Overnight cultures of bacterial strains encoding *lacZ* inserted at attB were diluted 1:100 in LB, grown to mid-log phase, and induced for one hour with 0.02% (*w/v*) arabinose or incubated with the pore-forming protein control (5 μM pyocin S5). Bacterial cells equivalent to 1 mL at $OD_{600}=0.5$ were collected by centrifugation and washed twice with 1 mL PBS. Cells were resuspended in 1 mL PBS, diluted 1:10 into PBS containing 2 mM *o*-nitrophenyl-β-glactoside (ONPG, Research Products International, Mount Prospect, IL), and shaken at 37°C for 1.5 hours. Absorbance at 420 nm was then measured to quantify ONPG turnover by intracellular β-galactosidase.

Membrane potential studies

Overnight cultures of bacterial strains were diluted 1:100 in LB medium, grown to mid-log phase, and induced with 0.02% (*w/v*) arabinose for one hour. Cells were pelleted by centrifugation and the OD_{600} set to 1. Cells (10 μl) were added to a staining mixture containing 30 μM $DiOC_2(3)$[19] (Thermo Fisher) and 5 mM EDTA ± 5 μM carbonyl cyanide *m*-chlorophenyl hydrazine (CCCP, Sigma-Aldrich) and incubated at room temperature for 10 minutes in the dark. Samples were analyzed on a BD LRSII flow cytometer with excitation at 488 nm and reading emission using GFP 530/30 (505 LP) and BV605 610/20 (585 LP). We recorded 10,000 events and gated out forward scatter and side scatter outliers before data analysis (between 300-700 events were removed). The red/green (BV605/GFP) fluorescence intensity values for each population were determined.

Intracellular pH assays

The pH-sensitive protein pHluorin2 (a GFP derivative) was used to monitor intracellular pH levels[20]. This protein was expressed in *P. aeruginosa* via IPTG induction from the plasmid pPSV39-CV::*pHluorin2*. Overnight cultures of strains carrying this plasmid were diluted 1:100 in LB medium with 0.2 mM IPTG, grown to mid-log phase, then treated with 0.02% (*w/v*) arabinose for one hour to induce Tse4 production. Cells were pelleted by centrifugation and duplicate samples were resuspended to $OD_{600}=2.5$ in 200 mM potassium phosphate buffer at each of the following pHs: 5.7, 6.3, 7, and 8. 40 mM sodium benzoate was added to one sample at each pH (positive control for proton motive force disruption), while the second sample was untreated. After 20 min, we then measured the ratio of absorbance at 392 and 470 nm; low intracellular pH is indicated by a decrease in the 392/470 nm absorbance ratio for pHluorin2.

Preparation of proteins and Western blotting

To co-purify Tse4 and Tsi4, an overnight culture of *E. coli* harboring pETDuet-1 (mcs1:: *tsi4-his6*, mcs2:: *vsv-g*-tse4) was diluted 1:200 in fresh media and incubated at 37°C until mid-log phase. Cultures were then induced with 0.5 mM ITPG, harvested 4 hours post-induction by centrifugation at 4,000 × g for 10 minutes, and pellets resuspended in 2 mL Wash Buffer (50 mM Tris-HCl pH 7.5, 500 mM NaCl, 2% glycerol) with 1 mg/mL lysozyme, 0.5 mg/mL DNase, and 1% Triton X-100. The resuspension was manually lysed through sonication, centrifuged at 4°C for 30 minutes at 16,000 × g, and lysates applied to

250 μL of Ni-NTA beads (Qiagen). Beads were incubated with rotation for 1 hour at 4°C, washed 3 times in 10 mL of Wash Buffer with 0.1% Triton X-100, and protein was eluted with 300 μL of Wash Buffer containing 500 mM imidazole pH 7.4 and 0.1% Triton X-100. For secretion assays, samples were prepared as previously described[31]. All proteins samples were analyzed by SDS-PAGE and Western blotting as previously described[32] using rabbit α-VSV-G (1:5000, Sigma) and mouse α-RNAP (1:5000, BioLegend) and then detected with α-rabbit and α-mouse horseradish peroxidase-conjugated antibodies (1:5000, Sigma). Western blots were developed using chemiluminescent substrate (SuperSignal West Pico Substrate, Thermo Scientific) and imaged with a FluorChemQ (ProteinSimple, San Jose, California). The original Western blot images are provided in Supplementary Fig. 5.

Statistics

All statistical tests were performed in GraphPad Prism 7.0 with $\alpha=0.05$; p-values less than 0.05 are indicated by asterisks (*).

Data availability

The authors declare that the data supporting the findings of this study are available within the paper and its supplementary information files.

Code availability

Computer code generated for this study is available upon request.

Supplementary Material

Refer to Web version on PubMed Central for supplementary material.

Acknowledgments

References

1. Stubbendieck RM, Straight PD. Multifaceted Interfaces of Bacterial Competition. J Bacteriol. 2016; 198:2145–2155. DOI: 10.1128/JB.00275-16 [PubMed: 27246570]

2. Hibbing ME, Fuqua C, Parsek MR, Peterson SB. Bacterial competition: surviving and thriving in the microbial jungle. Nat Rev Microbiol. 2010; 8:15–25. doi:nrmicro2259 [pii] 10.1038/nrmicro2259. [PubMed: 19946288]

3. Hood RD, Peterson SB, Mougous JD. From Striking Out to Striking Gold: Discovering that Type VI Secretion Targets Bacteria. Cell host & microbe. 2017; 21:286–289. DOI: 10.1016/j.chom. 2017.02.001 [PubMed: 28279332]

4. Hood RD, et al. A type VI secretion system of Pseudomonas aeruginosa targets a toxin to bacteria. Cell host & microbe. 2010; 7:25–37. [PubMed: 20114026]

5. Hachani A, Wood TE, Filloux A. Type VI secretion and anti-host effectors. Current opinion in microbiology. 2016; 29:81–93. DOI: 10.1016/j.mib.2015.11.006 [PubMed: 26722980]

6. Pukatzki S, Ma AT, Revel AT, Sturtevant D, Mekalanos JJ. Type VI secretion system translocates a phage tail spike-like protein into target cells where it cross-links actin. Proc Natl Acad Sci U S A. 2007; 104:15508–15513. [PubMed: 17873062]

7. Alcoforado Diniz J, Liu YC, Coulthurst SJ. Molecular weaponry: diverse effectors delivered by the Type VI secretion system. Cellular microbiology. 2015; 17:1742–1751. DOI: 10.1111/cmi.12532 [PubMed: 26432982]

8. Russell AB, Peterson SB, Mougous JD. Type VI secretion system effectors: poisons with a purpose. Nature reviews Microbiology. 2014; 12:137–148. DOI: 10.1038/nrmicro3185 [PubMed: 24384601]

9. Russell AB, et al. Type VI secretion delivers bacteriolytic effectors to target cells. Nature. 2011; 475:343–347. DOI: 10.1038/nature10244 [PubMed: 21776080]

10. Russell AB, et al. Diverse type VI secretion phospholipases are functionally plastic antibacterial effectors. Nature. 2013; 496:508–512. DOI: 10.1038/nature12074 [PubMed: 23552891]

11. Whitney JC, et al. An interbacterial NAD(P)(+) glycohydrolase toxin requires elongation factor Tu for delivery to target cells. Cell. 2015; 163:607–619. DOI: 10.1016/j.cell.2015.09.027 [PubMed: 26456113]

12. Durand E, Cambillau C, Cascales E, Journet L. VgrG, Tae, Tle, and beyond: the versatile arsenal of Type VI secretion effectors. Trends in microbiology. 2014; 22:498–507. DOI: 10.1016/j.tim. 2014.06.004 [PubMed: 25042941]

13. Fischbach MA. Combination therapies for combating antimicrobial resistance. Current opinion in microbiology. 2011; 14:519–523. DOI: 10.1016/j.mib.2011.08.003 [PubMed: 21900036]

14. Goodman AL, et al. A signaling network reciprocally regulates genes associated with acute infection and chronic persistence in Pseudomonas aeruginosa. Dev Cell. 2004; 7:745–754. [PubMed: 15525535]

15. Leroux M, et al. Quantitative single-cell characterization of bacterial interactions reveals type VI secretion is a double-edged sword. Proceedings of the National Academy of Sciences of the United States of America. 2012; 109:19804–19809. DOI: 10.1073/pnas.1213963109 [PubMed: 23150540]

16. Whitney JC, et al. Genetically distinct pathways guide effector export through the type VI secretion system. Molecular microbiology. 2014; 92:529–542. DOI: 10.1111/mmi.12571 [PubMed: 24589350]

17. Casabona MG, Vandenbrouck Y, Attree I, Coute Y. Proteomic characterization of Pseudomonas aeruginosa PAO1 inner membrane. Proteomics. 2013; 13:2419–2423. DOI: 10.1002/pmic. 201200565 [PubMed: 23744604]

18. Kim S, et al. Transmembrane glycine zippers: physiological and pathological roles in membrane proteins. Proc Natl Acad Sci U S A. 2005; 102:14278–14283. DOI: 10.1073/pnas.0501234102 [PubMed: 16179394]

19. Hoffman JF, Laris PC. Determination of membrane potentials in human and Amphiuma red blood cells by means of fluorescent probe. J Physiol. 1974; 239:519–552. [PubMed: 4851321]

20. Mahon MJ. pHluorin2: an enhanced, ratiometric, pH-sensitive green florescent protein. Adv Biosci Biotechnol. 2011; 2:132–137. DOI: 10.4236/abb.2011.23021 [PubMed: 21841969]

21. Rice KC, Bayles KW. Death's toolbox: examining the molecular components of bacterial programmed cell death. Mol Microbiol. 2003; 50:729–738. [PubMed: 14617136]

22. Baym M, Stone LK, Kishony R. Multidrug evolutionary strategies to reverse antibiotic resistance. Science. 2016; 351:aad3292. [PubMed: 26722002]

23. Stover CK, et al. Complete genome sequence of Pseudomonas aeruginosa PA01, an opportunistic pathogen. Nature. 2000; 406:959–964. [PubMed: 10984043]

24. Hoang TT, Kutchma AJ, Becher A, Schweizer HP. Integration-proficient plasmids for Pseudomonas aeruginosa: site-specific integration and use for engineering of reporter and expression strains. Plasmid. 2000; 43:59–72. [PubMed: 10610820]

25. Kulasekara BR, et al. c-di-GMP heterogeneity is generated by the chemotaxis machinery to regulate flagellar motility. Elife. 2013; 2:e01402. [PubMed: 24347546]

26. Ma LS, Hachani A, Lin JS, Filloux A, Lai EM. Agrobacterium tumefaciens deploys a superfamily of type VI secretion DNase effectors as weapons for interbacterial competition in planta. Cell host & microbe. 2014; 16:94–104. DOI: 10.1016/j.chom.2014.06.002 [PubMed: 24981331]

27. Miyata ST, Unterweger D, Rudko SP, Pukatzki S. Dual expression profile of type VI secretion system immunity genes protects pandemic Vibrio cholerae. PLoS Pathog. 2013; 9:e1003752. [PubMed: 24348240]

28. Russell AB, et al. A widespread bacterial type VI secretion effector superfamily identified using a heuristic approach. Cell host & microbe. 2012; 11:538–549. DOI: 10.1016/j.chom.2012.04.007 [PubMed: 22607806]

29. Whitney JC, et al. Identification, Structure, and Function of a Novel Type VI Secretion Peptidoglycan Glycoside Hydrolase Effector-Immunity Pair. The Journal of biological chemistry. 2013; 288:26616–26624. DOI: 10.1074/jbc.M113.488320 [PubMed: 23878199]

30. Rietsch A, Vallet-Gely I, Dove SL, Mekalanos JJ. ExsE, a secreted regulator of type III secretion genes in Pseudomonas aeruginosa. Proc Natl Acad Sci U S A. 2005; 102:8006–8011. [PubMed: 15911752]

31. Silverman JM, et al. Separate inputs modulate phosphorylation-dependent and -independent type VI secretion activation. Mol Microbiol. 2011; 82:1277–1290. DOI: 10.1111/j.1365-2958.2011.07889.x [PubMed: 22017253]

32. Mougous JD, et al. A virulence locus of Pseudomonas aeruginosa encodes a protein secretion apparatus. Science. 2006; 312:1526–1530. [PubMed: 16763151]

33. Vance RE, Rietsch A, Mekalanos JJ. Role of the type III secreted exoenzymes S, T, and Y in systemic spread of Pseudomonas aeruginosa PAO1 in vivo. Infection and immunity. 2005; 73:1706–1713. [PubMed: 15731071]

34. Pansegrau W, et al. Complete nucleotide sequence of Birmingham IncP alpha plasmids. Compilation and comparative analysis. J Mol Biol. 1994; 239:623–663. DOI: 10.1006/jmbi.1994.1404 [PubMed: 8014987]

35. Silverman JM, et al. Haemolysin Coregulated Protein Is an Exported Receptor and Chaperone of Type VI Secretion Substrates. Molecular cell. 2013; 51:584–593. DOI: 10.1016/j.molcel.2013.07.025 [PubMed: 23954347]
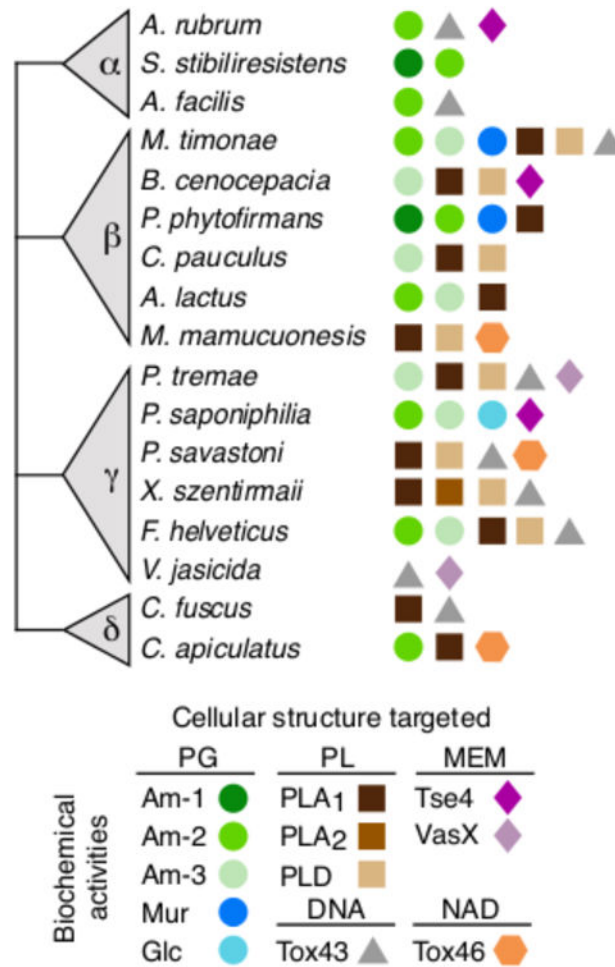
Fig. 1. Diverse species of Gram-negative bacteria encode multiple T6SS effectors with distinct biochemical activities

Shown are select results of a custom search algorithm used to identify orthologs of biochemically characterized T6SS effectors in all sequenced Proteobacterial species (complete results provided in Supplemental Table 1). Symbols signify characterized effector activities found in the genome of the indicated species. Target molecules (shape) and distinct biochemical activities (color shade) are denoted. Abbreviations: PG, peptidoglycan; PL, phospholipids; MEM, membranes; Am, amidase; Mur, muramidase; Glc, *N*-acetylglucosamidase; PLA, phospholipase A; PLD, phospholipase.
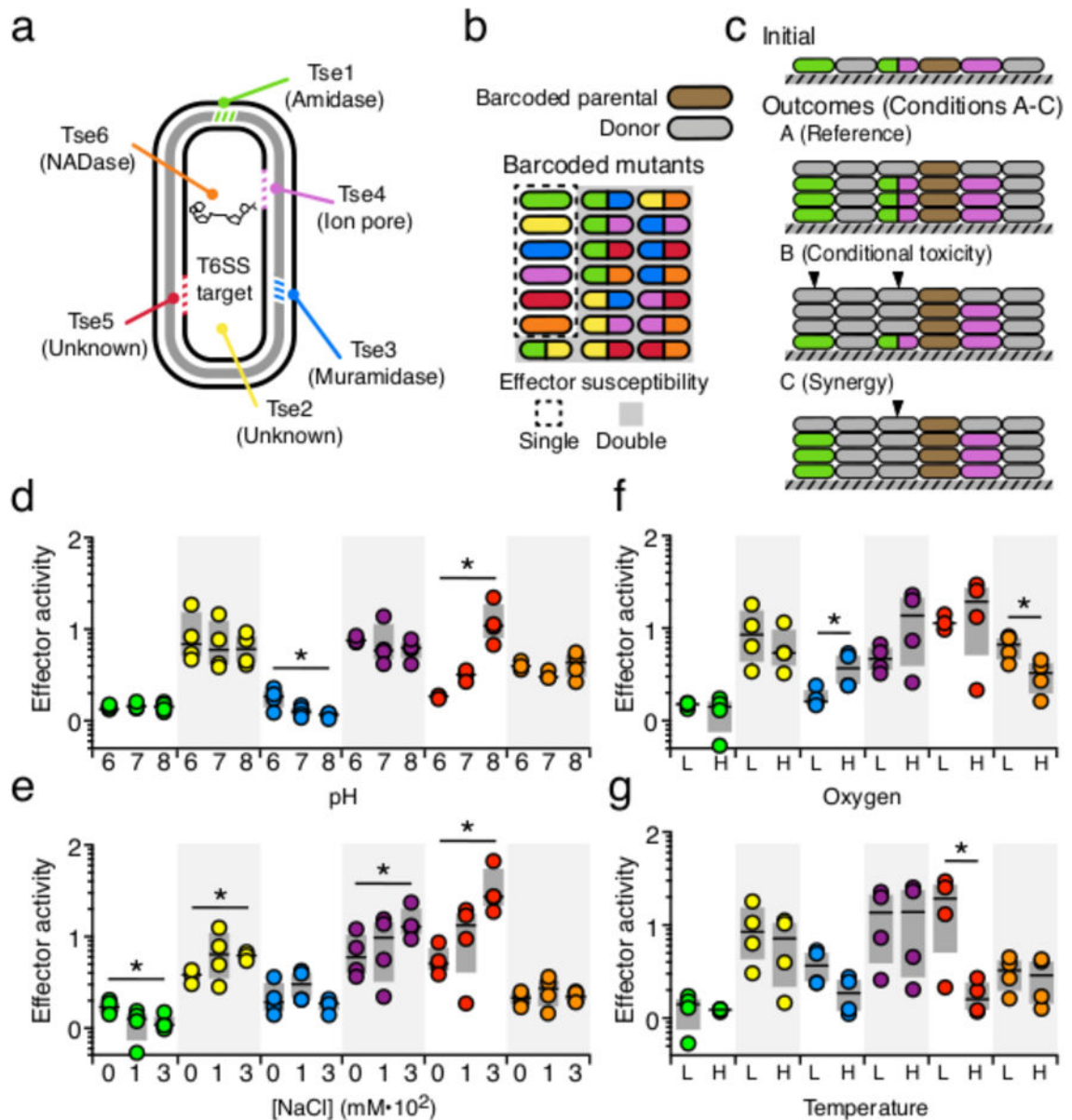
Fig. 2. Parallel analysis of effector efficacy (PAEE) reveals that environmental conditions influence the potency of T6SS effectors

a, Diagram indicating cellular compartment in which each H1-T6SS effector of *P. aeruginosa* acts, and their biochemical activities, when known. **b**, Representation of the pool of strains employed in PAEE. Colors indicate effector susceptibility of each strain (Tse1-Tse6 colors correspond to Fig. 2a; barcoded parental, brown; unbarcoded donor, grey). Effector susceptibility color scheme is employed throughout subsequent figures. **c**, Simplified depiction of potential outcomes following competition of a donor strain and recipient strains susceptible to one or both of two effectors with conditional differences in activity (A vs. B) or conditional synergy (A vs. C). Arrowheads indicate mutants with increased toxin susceptibility in comparison to the reference condition. **d-g**, Relative activity of *P. aeruginosa* H1-T6SS effectors under assorted growth conditions as determined by

PAEE (n=4 biologically independent experiments). Effector activity is calculated by comparing the ratios of the barcoded parental to mutants susceptible to each effector before and after growth of the pooled population. Grey boxes enclose the 25-75 percentile range and bars represent the median value. *P<0.05 (ratio paired t-test between each condition). Conditions varied include pH (**d**), NaCl levels (**e**), oxygen availability (H vs. L oxygen) (**f**), and temperature (**g**) (42˚C, H vs. 37˚C, L).
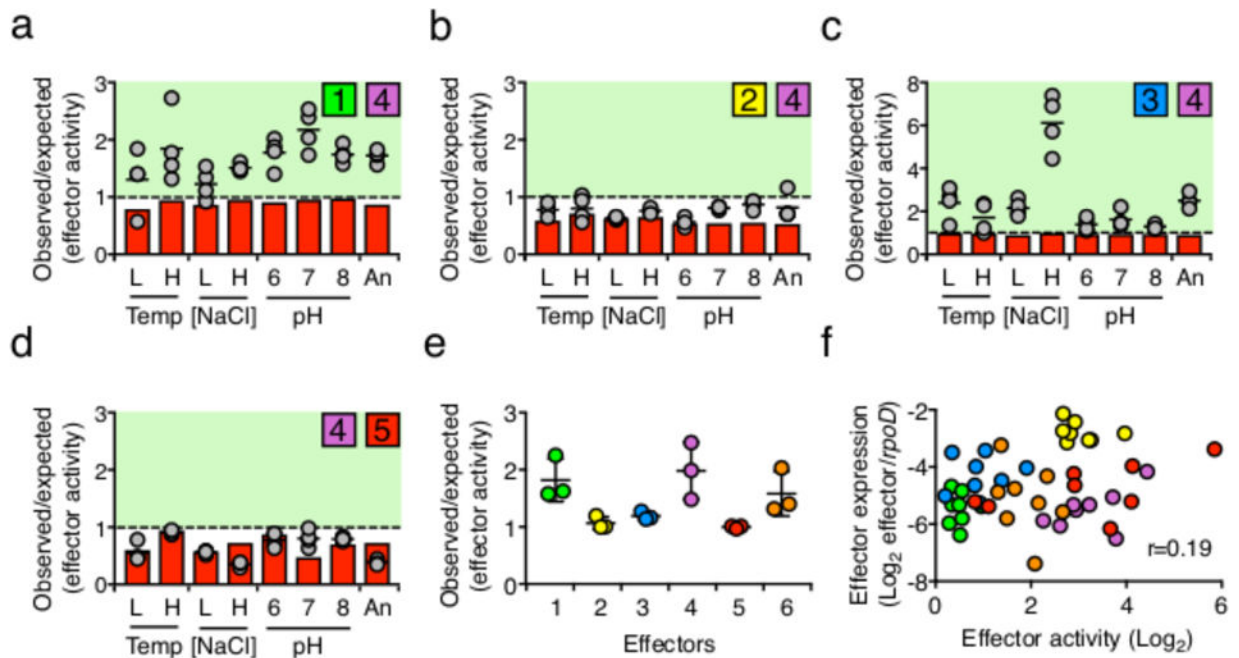
Fig. 3. Environmental conditions and effector activities influence synergy between T6SS effectors
a-d, Filled circles indicate observed (in PAEE screen):expected (sum of individual effector activities measured by PAEE) activity for the indicated effector pairs. Ratios reflecting synergistic (green) or inhibitory (red) interactions are indicated. Single and paired effector activities calculated as in Fig. 2. Inhibitory interactions for each effector pair calculated as the portion of the additive effect that is contributed by the more active effector (red bars). Values between red bars and dashed line are additive. High temperature (H), 42°C, low (L), 37°C; high NaCl, 300 mM, low, 0 mM. (n=4 biologically independent experiments). **e**, Average observed:expected activity for the indicated effectors paired with each other effector under a given condition. Measurements are plotted only for the conditions with the three highest average observed:expected values for a given effector. **f**, Effector expression levels (as measured by qRT-PCR, n=3 biologically independent experiments) plotted against effector activity level (as determined by PAEE, n=4 biologically independent experiments) under the same set of conditions. Colors indicate effector identity (see Fig. 2). Pearson's correlation coefficient is indicated. **a-e**, Data presented as mean values ± standard deviation (**e**).
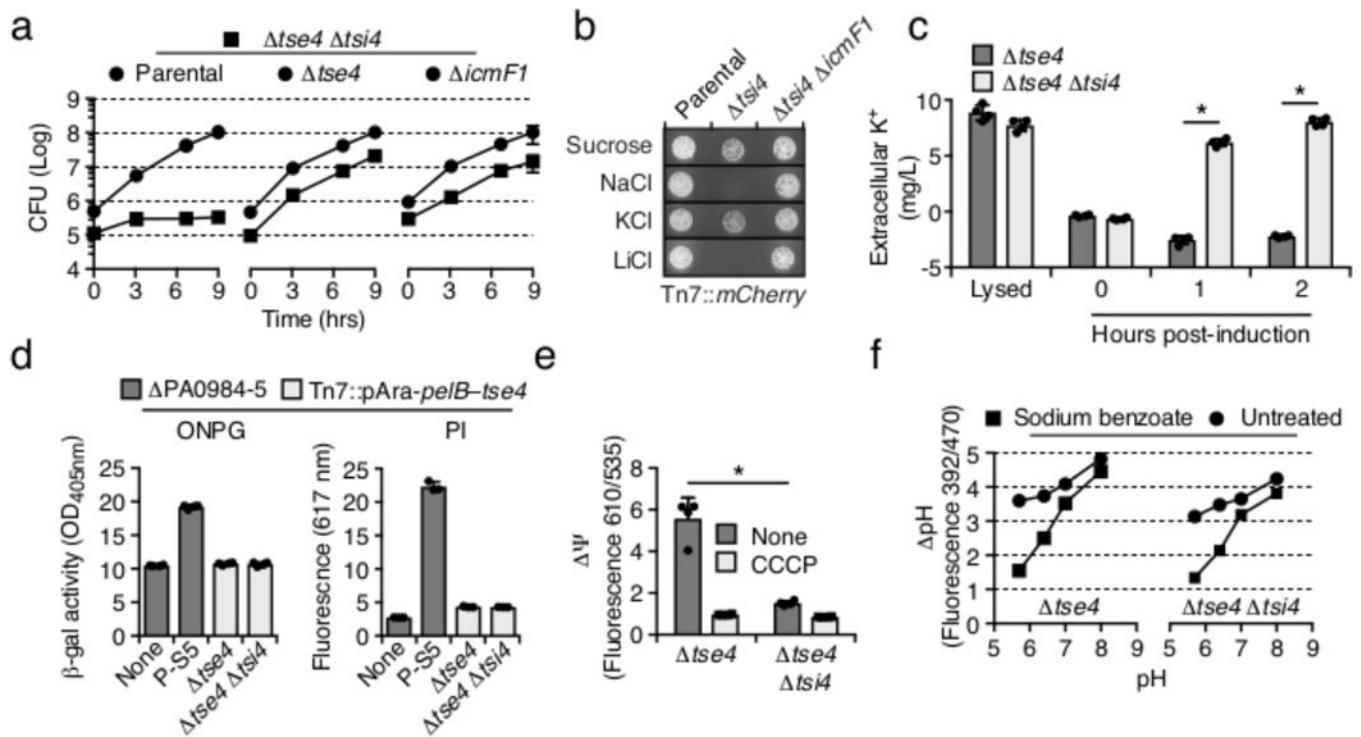
Fig. 4. A synergistic T6SS effector of previously unknown function introduces ion permeability
a, Growth of a Tse4-susceptible strain (tse4 tsi4) and the indicated co-cultured strains on solid medium (n=3 biologically independent samples) **b**, Growth of the specified strains after 16 hrs incubation on solid growth medium supplemented with the indicated solutes (sucrose, 300 mM; NaCl, 150 mM; KCl, 150 mM; LiCl, 20 mM). Cells were visualized through mCherry fluorescence. This experiment was repeated independently five times with similar results. **c-f**, Changes to membrane permeability assessed through ectopic, periplasmically-targeted expression of Tse4 (Tn7::pAra-*pelB–tse4*) in *P. aeruginosa* populations susceptible (tse4 tsi4) or resistant (tse4) to Tse4 intoxication. **c**, Extracellular K^+ levels measured in the supernatants of Tse4-expressing cultures (susceptible, light grey; resistant, dark grey) (n=4 biologically independent samples). Lysed cells provide the maximal concentration that can be released. **d**, Intracellular uptake of ONPG or PI by cells rendered genetically susceptible to the non-selective pore-forming toxin pyocin S5 (dark grey bars) or by cells expressing Tse4 (light grey bars) (n=3 biologically independent samples). ONPG uptake monitored through intracellular β-galactosidase-meditated release of *o*-nitrophenol (OD 405 nm); PI uptake monitored through intracellular fluorescence (617 nm). **e**, Membrane polarization of Tse4-expressing cultures (n=3 biologically independent samples). CCCP-treated cultures (light grey) included as depolarized controls. Membrane potential is indicated by the ratio of fluorescence intensities (610/535 nm) emitted by cells treated with $DiOC_2(3)$. **f**, Intracellular pH change in Tse4-expressing cells incubated in buffers of varying pH (n=3 biologically independent samples). Sodium benzoate treated populations included as a control for proton gradient dissipation. Intracellular pH indicated by ratio of excitation peaks (392/470 nm) exhibited by pHluorin2

expressed by each population. **a, c-f**, Data presented as mean values ± standard deviation (error bars in **f** not visible due to overlap with symbols) *P<0.05 (two-tailed t-test).